Electronic Supplementary Information

Experimental Section

Materials: Sodium nitrite ($NaNO_2$), trisodium citrate dihydrate ($C_6H_5Na_3O_7 \cdot 2H_2O$), and sodium hypochlorite solution (NaClO) were purchased from Fuchen Chemical Reagent Co. Ltd. Sodium hydroxide (NaOH), ammonium chloride (NH_4Cl), salicylic acid ($C_7H_6O_3$), sodium nitroferricyanide dihydrate ($C_5FeN_6Na_2O \cdot 2H_2O$), and p-dimethylaminobenzaldehyde (p-$C_9H_{11}NO$) were purchased from Aladdin Ltd. Zinc chloride ($ZnCl_2$) was purchased from Maclin Biochemical Co. Ltd (Shanghai, China). Iron nitrate hexahydrate ($Fe(NO_3)_3 \cdot 9H_2O$), urea (CH_4N_2O), and ammonium fluoride (NH_4F) were purchased from Chengdu Kelong Chemical Reagent Factory. Ethyl alcohol (C_2H_5OH) and hydrazine hydrate ($N_2H_4 \cdot H_2O$) were provided by Beijing Chemical Works. Hydrochloric acid (HCl) was bought from Keshi Chemical Reagent Co. Nickel foam (NF) was provided by Suzhou Tali New Energy Co. Ltd. All chemical regents were used as received without further purification. Ultrapure (up) water was made by the Millipore system and used in all experimental process.

Synthesis of $ZnFe_2O_4$/NF and Fe_3O_4/NF: NF (2.0 × 3.0 cm^2) was ultrasonic cleaned with HCl, C_2H_5OH, and up water for 15 min before use to remove surface oxide layer. Firstly, 0.14 g $ZnCl_2$, 0.80 g $Fe(NO_3)_3 \cdot 9H_2O$, 0.15 g NH_4F, and 0.72 g CH_4N_2O were dissolved in 60 mL up water and stirred for 15 min. The blended solution was then poured into an 80 mL Teflon-lined autoclave and placed into the treated NF. Afterwards, the autoclave was kept in an oven at 120 °C for 6 h. After cooling to room temperature, the precursor material was removed and ultrasonic cleaned with up water and C_2H_5OH. After drying, the $ZnFe_2O_4$/NF nanosheet array was finally obtained by calcining in muffle furnace at a heating rate of 2 °C/min from room temperature to 450 °C for 2 h. Similarly, Fe_3O_4/NF was synthesized in the same way without adding $ZnCl_2$.

Characterizations: XRD data were acquired by a LabX XRD–6100 X-ray diffractometer (SHIMADZU, Japan). SEM measurements were carried out on a GeminiSEM 300 (ZEISS, Germany). TEM (JEM-F200, JEOL Ltd.) was utilized to

further observe the micro-structure of materials. XPS measurements were performed on an ESCALABMK II X-ray photoelectron spectrometer. The absorbance data of products were collected by UV-vis spectrophotometer (Shimadzu UV-2700). The gas by-products were quantitatively detected by Gas chromatography (GC-2014C, SHIMADZU).

Electrochemical measurements: The entire electrochemical measurements were carried out using a CHI 760E electrochemical analyzer (Chenhua, Shanghai) in an H-type electrolytic cell separated by a Nafion 117 ion exchange membrane. In a typical three-electrode system, $ZnFe_2O_4$/NF, Fe_3O_4/NF, and NF (1 × 0.5 cm^2) were used as working electrode, graphite rod as counter electrode, and Hg/HgO electrode as reference electrode, respectively. LSV was performed at a scan rate of 5 mV s^{-1} from 0.2 V to −1.0 V in 0.1 M NaOH with or without 0.1 M NO_2^- (70 mL). The potential was referenced to that of reversible hydrogen electrode (RHE), using the following equation: E (RHE) = E (Hg/HgO) + (0.098 + 0.059 × pH) V. To assess the ESCA of the electrocatalyst, cyclic voltammetry (CV) curves were performed at scan rates of 0.01–0.1 V s^{-1} in 0.1 M NaOH with or without 0.1 M NO_2^-. Electrochemical impedance spectra (EIS) were measured in a frequency domain ranging from 0.1 Hz to 10^6 Hz with 5 mV amplitude.

Determination of NH_3: The concentration of produced NH_3 was determined by spectrophotometry measurement with indophenol blue method.[1] In detail, 2 mL of diluted 50 times catholyte was derived from cathode chamber and mixed with 2 mL of 1 M NaOH solution containing $C_7H_6O_3$ (5 wt%) and $C_5FeN_6Na_2O{\cdot}2H_2O$ (5 wt%). Then, 1 mL of 0.05 M NaClO and 200 μL of $C_5FeN_6Na_2O$ (1 wt%) were dropped in the collected electrolyte solution. After standing at room temperature for 2 h, the UV-vis absorption spectrum was measured. The concentration-absorbance curve was calibrated using the standard NH_4Cl solution with NH_3 concentrations of 0, 0.2, 0.25, 0.5, 0.75, 1.5, 2.0, and 5.0 ppm in 0.1 M NaOH. The absorbance at 655 nm was measured to quantify the NH_3 concentration using standard NH_4Cl solutions ($y = 0.43121x + 0.00462$, $R^2 = 0.999$).

Determination of N_2H_4: In this work, the concentration of produced N_2H_4 was

measured by Watt and Chrisp method[2]. The color reagent was a mixed solution of 4.0 g $C_9H_{11}NO$, 24 mL HCl (37%), and 200 mL C_2H_5OH. In detail, 2 mL electrolyte was added into 2 mL prepared color reagent and stirred for 15 min in the dark. The absorbance at 455 nm was measured to quantify the N_2H_4 concentration with a standard curve of N_2H_4 ($y = 0.62783x + 0.00767$, $R^2 = 0.999$).

Calculations of FE and NH_3 yield:

$$FE = (6 \times F \times [NH_3] \times V) / (M_{NH_3} \times Q) \times 100\%$$

$$NH_3 \text{ yield} = ([NH_3] \times V) / (t \times A)$$

Where F is the Faradic constant (96485 C mol^{-1}), $[NH_3]$ is the measured NH_3 concentration, V is the volume of electrolyte (70 mL), M_{NH_3} is the molar mass of NH_3, Q is the total charge passing though the electrode, t is the electrolysis time, and A is the geometric area of working electrode (0.5 × 1.0 cm^2).

Calculations of $j_{partial}$:

The partial current density of NH_3 ($j_{partial}$) was calculated as:

$$j_{partial} = FE \times I_{it}$$

which FE for each product, I_{it} is the average current density (mA cm^{-2}).

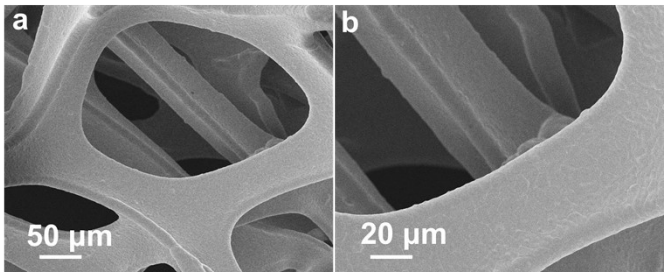

Fig. S1. SEM images of NF.

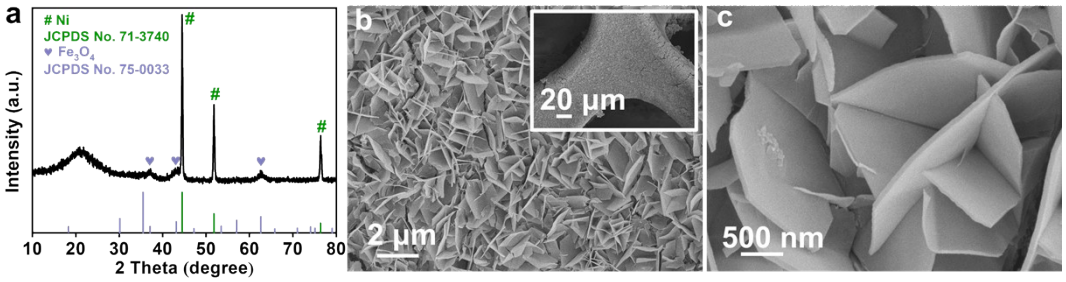

Fig. S2. (a) XRD pattern and (b, c) SEM images for Fe_3O_4/NF.

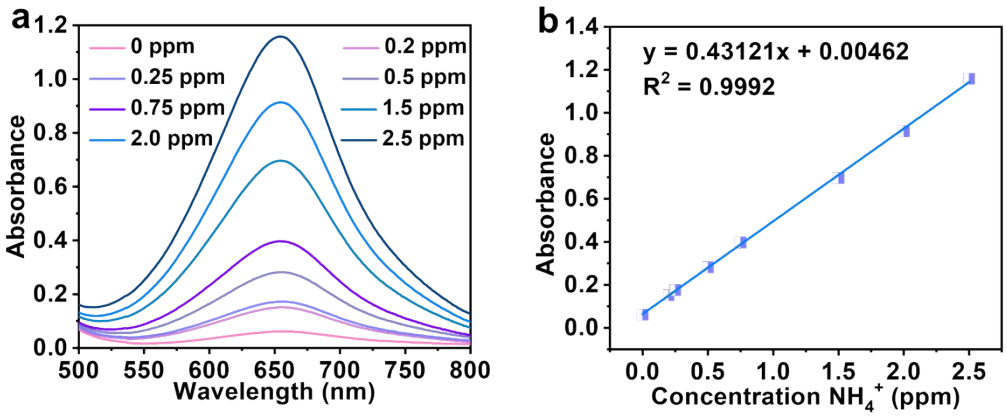

Fig. S3. (a) UV-vis absorption spectra of different NH_4^+ concentrations after incubated for 2 h at room temperature. (b) Calibration curve used for estimation of NH_4^+ concentration.

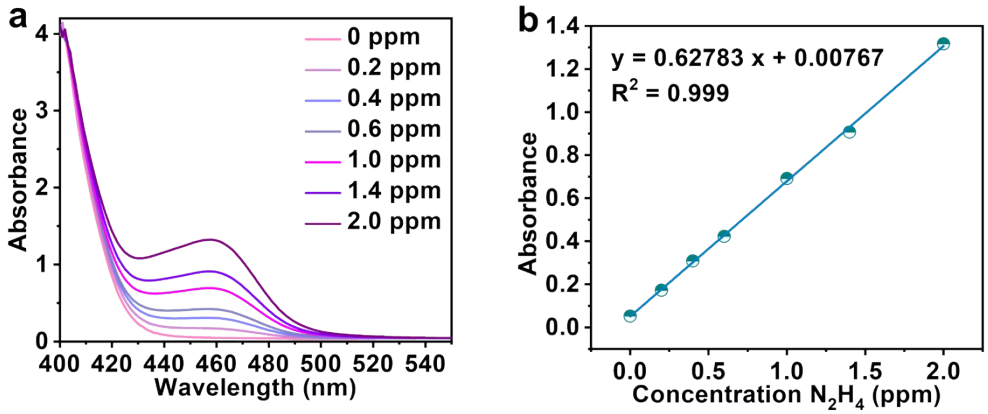

Fig. S4. (a) UV-vis absorption spectra of various N_2H_4 concentrations after incubated for 15 min at room temperature. (b) Calibration curve used for calculation of N_2H_4 concentration.

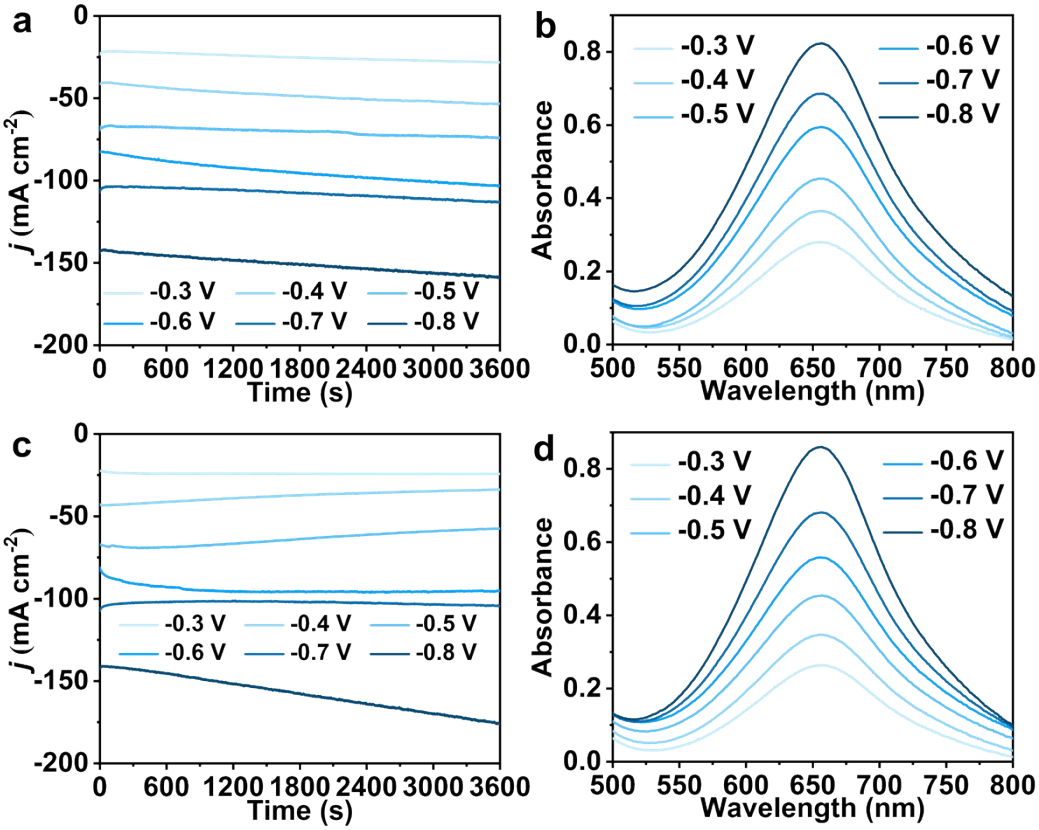

Fig. S5. (a, c) CA curves and (b, d) corresponding UV-vis spectra of $ZnFe_2O_4$/NF for another two separate tests at various applied potentials.

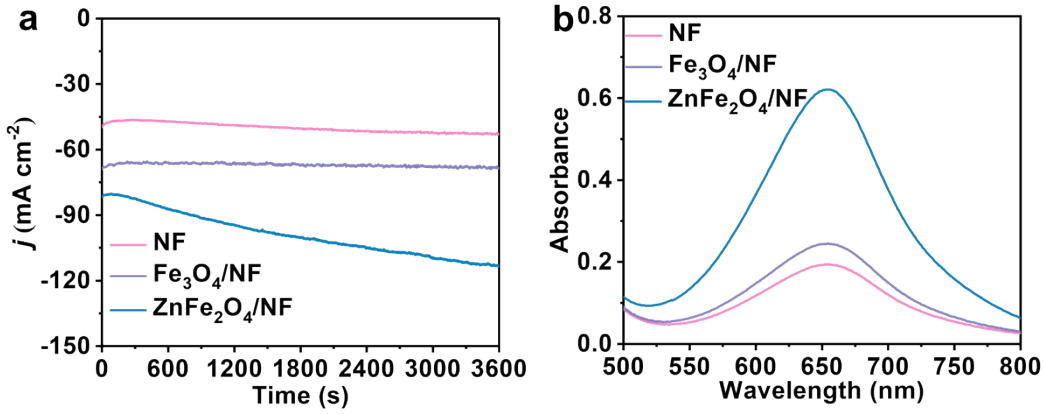

Fig. S6. (a) Time-dependent current density curves of NF, Fe_3O_4/NF, and $ZnFe_2O_4$/NF for eNO_2^-RR at –0.6 V and (b) corresponding UV-vis absorption spectra for calculation of NH_3 concentration.

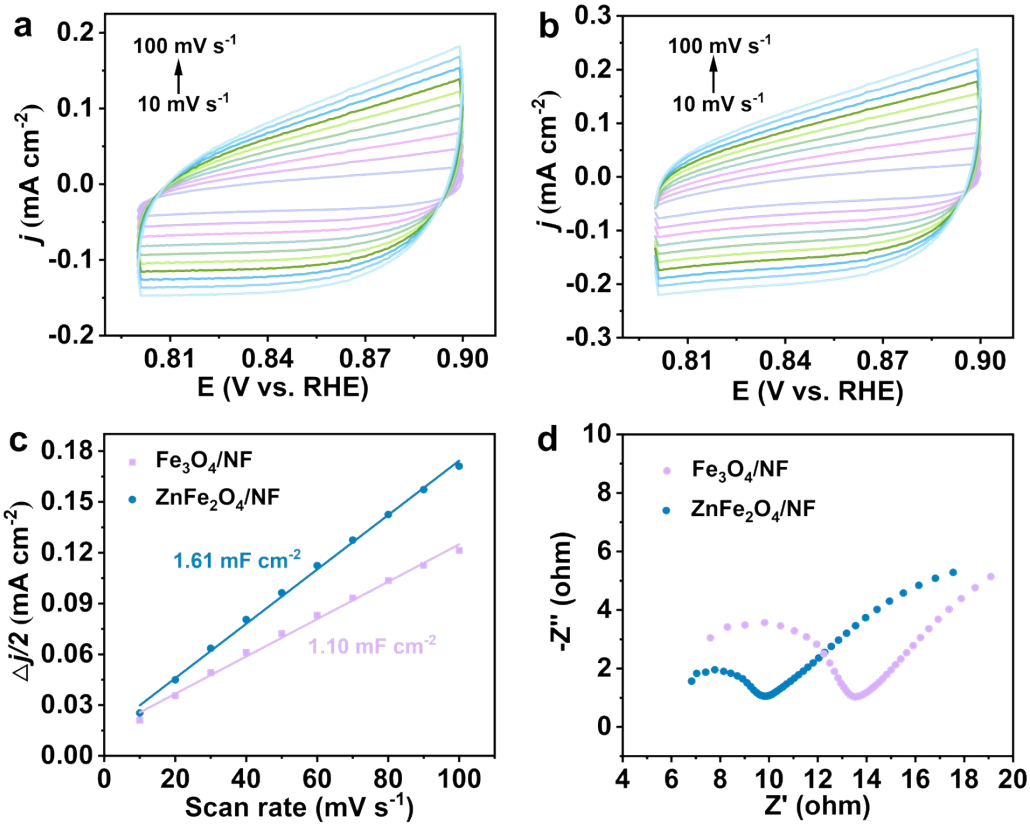

Fig. S7. Cyclic voltammograms of (a) Fe_3O_4/NF and (b) $ZnFe_2O_4$/NF. (c) Plots of capacitive currents densities verse scan rate. (d) Electrochemical impedance spectra of Fe_3O_4/NF and $ZnFe_2O_4$/NF.

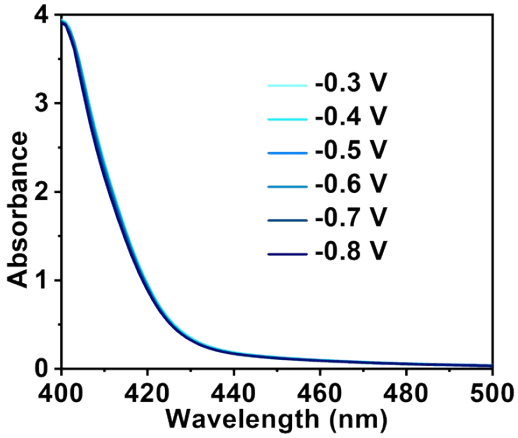

Fig. S8. UV-vis absorption spectra of N_2H_4 detection.

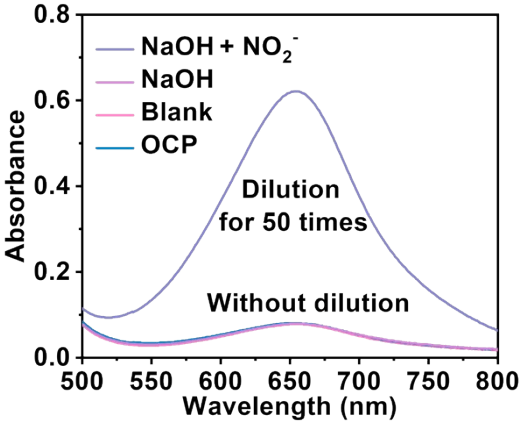

Fig. S9. UV-vis absorption spectra of the amount of produced NH_3 of $ZnFe_2O_4$/NF via eNO_2^-RR at different conditions.

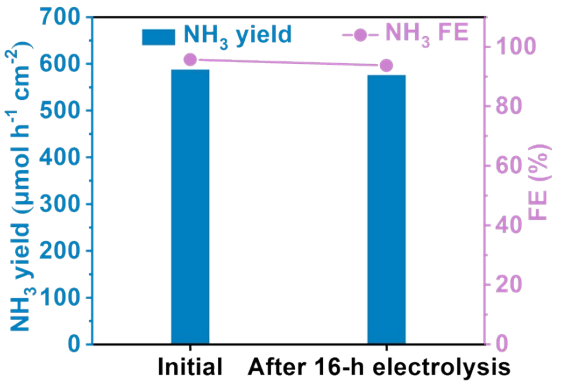

Fig. S10. NH_3 yields and FEs of $ZnFe_2O_4$/NF before and after 16-h electrolysis.

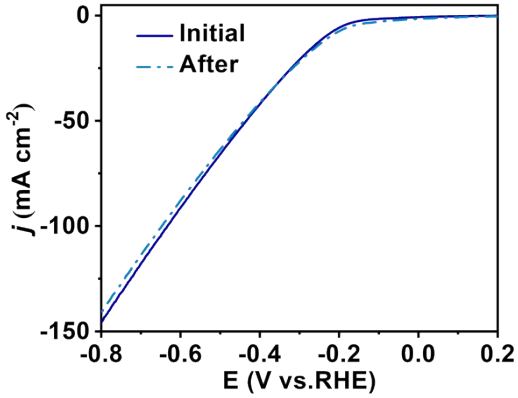

Fig. S11. LSV curves of $ZnFe_2O_4$/NF before and after 16-h electrolysis.

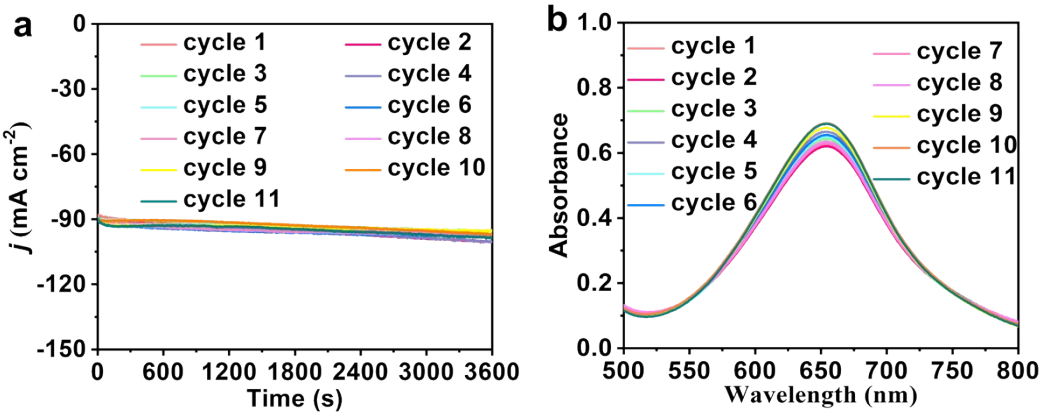

Fig. S12. (a) Chronoamperometry curves for $ZnFe_2O_4$/NF during recycling tests toward eNO_2^-RR at −0.6 V and (b) corresponding UV-vis absorption spectra for electrogenerated NH_3.

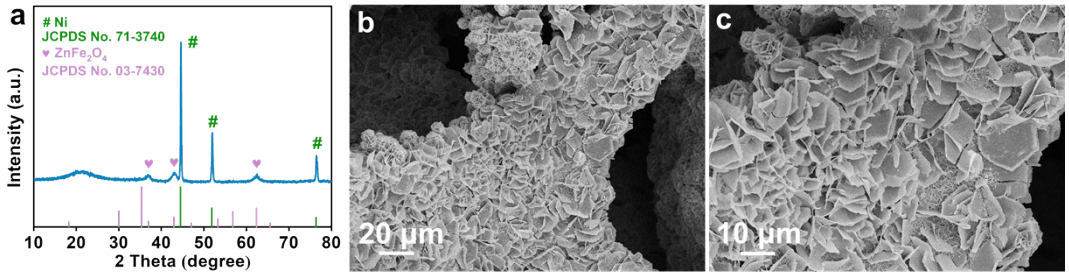

Fig. S13. (a) XRD pattern and (b, c) SEM images of $ZnFe_2O_4$/NF after 16-h electrolysis.

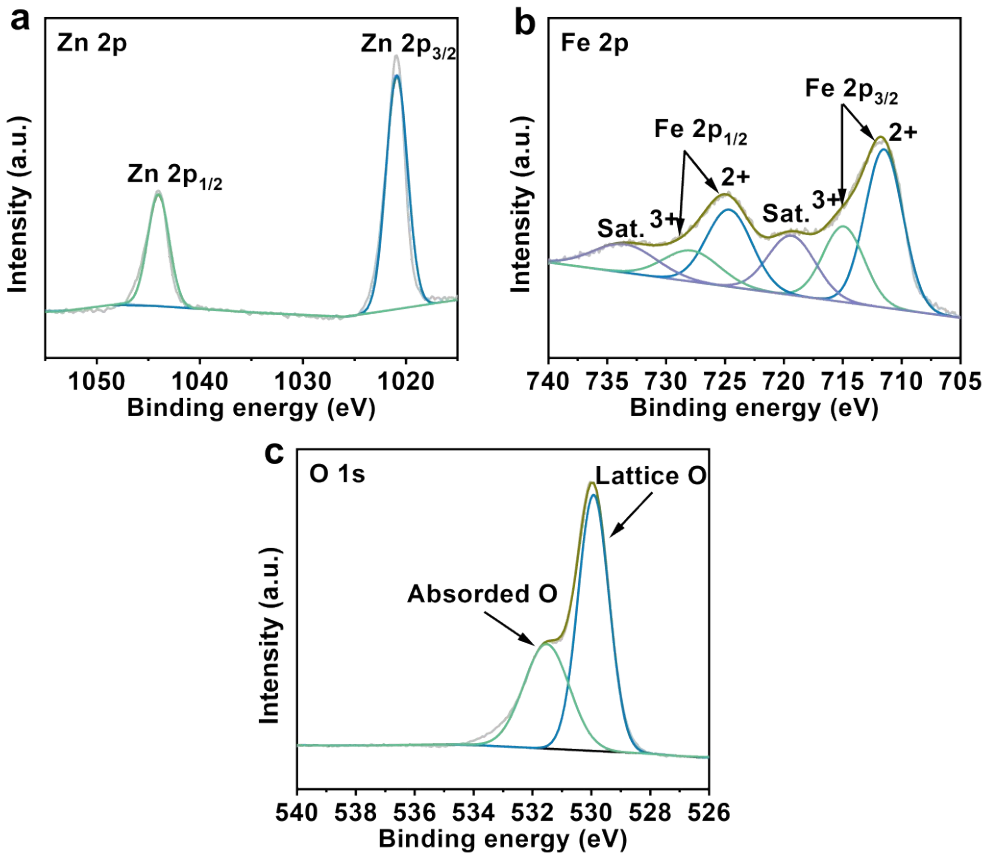

Fig. S14. XPS spectra in the (a) Zn 2p, (b) Fe 2p, and (c) O 1s regions of $ZnFe_2O_4$ after 16-h electrolysis.

Table S1. Comparison of catalytic performance of $ZnFe_2O_4$/NF with other reported eNO_2^-RR electrocatalysts.

Catalyst	Eletrolyte	NH_3 yield ($\mu mol\ h^{-1}cm^{-2}$)	FE (%)	Ref.
$ZnFe_2O_4$/NF	0.1 M NaOH (0.1 M NO_2^-)	588.58	95.7	This work
TiO_{2-x} NBA/TP	0.1 M NaOH (0.1 M NO_2^-)	464.6	92.7	(3)
Ag@NiO/CC	0.1 M NaOH (0.1 M NO_2^-)	338.3	97.7	(4)
Cu/JDC/CP	0.1 M NaOH (0.1 M NO_2^-)	523.5	93.2	(5)
FeP@TiO_2/TP	0.1 M NaOH (0.1 M NO_2^-)	346.6	97.1	(6)
FeOOH NTA/CC	0.1 M PBS (0.1 M NO_2^-)	702.2	94.7	(7)
Ni@MDC	0.1 M NaOH (0.1 M NO_2^-)	300	65.4	(8)
Ni-TiO_2/TP	0.1 M NaOH (0.1 M NO_2^-)	380.3	94.9	(9)
Ni-NSA-V_{Ni}	0.2 M Na_2SO_4 (200 ppm NO_2^-)	235.5	88.9	(10)
NiS_2@TiO_2/TM	0.1 M NaOH (0.1 M NO_2^-)	454.3	92.1	(11)
WO_2/W	0.1 M NaOH (0.1 M NO_2^-)	880.25	94.32	(12)
CoFe-NC	0.1 M PBS (0.1 M NO_2^-)	238.3	94.5	(13)

CF@Cu_2O	0.1 M PBS (0.1 M NO_2^-)	441.81	94.21	(14)
CoB@TiO_2/TP	0.1 M Na_2SO_4 (400 ppm NO_2^-)	233.1	95.2	(15)
MoO_2/MP	0.5 M Na_2SO_4 (0.1 M NO_2^-)	510.5	94.5	(16)
CoP NA/TM	0.1 M PBS (500 ppm NO_2^-)	136.01	92.3	(17)
Ni_2P/NF	0.1 M PBS (200 ppm NO_2^-)	199.72	90.2	(18)
P-TiO_2/TP	0.1 M Na_2SO_4 (0.1 M NO_2^-)	560.8	90.6	(19)
V-TiO_2/TP	0.1 M NaOH (0.1 M NO_2^-)	540.8	93.2	(20)
Ru-Cu NW/CF	0.1 M PBS (500 ppm NO_2^-)	732	94.1	(21)
CoP/CC	1.0 M NaOH (2 mM NO_2^-)	22.35	91.6	(22)
Ni foam/TP	0.1 M PBS (0.1 M NO_2^-)	742.7	90.1	(23)
Nb−NiO	0.5 M Na_2SO_4 (0.1 M NO_2^-)	200.5	92.4	(24)

References

1 D. Zhu, L. Zhang, R. E. Ruther and R. J. Hamers, *Nat. Mater.*, 2013, **12**, 836–841.

2 G. W. Watt and J. D. Chrisp, *Anal. Chem.*, 1952, **24**, 2006–2008.

3 D. Zhao, J. Liang, J. Li, L. Zhang, K. Dong, L. Yue, Y. Luo, Y. Ren, Q. Liu, M. S. Hamdy, Q. Li, Q. Kong and X. Sun, *Chem. Commun.*, 2022, **58**, 3669–3672.

4 Q. Liu, G. Wen, D. Zhao, L. Xie, S. Sun, L. Zhang, Y. Luo, A. A. Alshehri, M. S. Hamdy, Q. Kong and X. Sun, *J. Colloid Interface Sci.*, 2022, **623**, 513–519.

5 L. Ouyang, L. Yue, Q. Liu, Q. Liu, Z. Li, S. Sun, Y. Luo, A. A. Alshehri, M. S. Hamdy, Q. Kong and X. Sun, *J. Colloid Interface Sci.*, 2022, **624**, 394–399.

6 A. Zhang, Y. Liang, X. He, X. Fan, C. Yang, L. Ouyang, D. Zheng, S. Sun, Z. Cai, Y. Luo, Q. Liu, S. Alfaifi, L. Cai, H. Wang and X. Sun, *Inorg. Chem.*, 2023, **62**, 12644–12649.

7 Q. Liu, Q. Liu, L. Xie, L. Yue, T. Li, Y. Luo, N. Li, B. Tang, L. Yu and X. Sun, *Chem. Commun.*, 2022, **58**, 5160–5163.

8 X. He, X. Li, X. Fan, J. Li, D. Zhao, L. Zhang, S. Sun, Y. Luo, D. Zheng, L. Xie, A. M. Asiri, Q. Liu and X. Sun, *ACS Appl. Nano Mater.*, 2022, **5**, 14246–14250.

9 Z. Cai, C. Ma, D. Zhao, X. Fan, R. Li, L. Zhang, J. Li, X. He, Y. Luo, D. Zheng,

i. Y. Wang, B. Ying, S. Sun, J. Xu, Q. Lu and X. Sun, *Mater. Today Energy*, 2023, **31**, 101220.

10 C. Wang, W. Zhou, Z. Sun, Y. Wang, B. Zhang and Y. Yu, *J. Mater. Chem. A*, 2021, **9**, 239–243.

11 X. He, L. Hu, L. Xie, Z. Li, J. Chen, X. Li, J. Li, L. Zhang, X. Fang, D. Zheng, S. Sun, J. Zhang, A. A. Alshehri, Y. Luo, Q. Liu, Y. Wang and X. Sun, *J. Colloid Interface Sci.*, 2023, **634**, 86–92.

12 H. Qiu, Q. Chen, X. An, Q. Liu, L. Xie, J. Zhang, W. Yao, Y. Luo, S. Sun, Q. Kong, J. Chen and X. Sun, *J. Mater. Chem. A*, 2022, **10**, 24969–24974.

13 D. Zhu, B. Zhang, J. Chen, F. Xie, Y. Zou and P. Chen, *Chem. Commun.*, 2023, **59**, 9626–9629.

1. Q. Chen, X. An, Q. Liu, X. Wu, L. Xie, J. Zhang, W. Yao, M. S. Hamdy, Q. Kong and
X. Sun, *Chem. Commun.*, 2022, **58**, 517–520.
2. L. Hu, D. Zhao, C. Liu, Y. Liang, D. Zheng, S. Sun, Q. Li, Q. Liu, Y. Luo, Y. Liao, L. Xie and X. Sun, *Inorg. Chem. Front.*, 2022, **9**, 6075–6079.
3. G. Wang, Q. Chen, X. An, Q. Liu, L. Xie, J. Zhang, W. Yao, X. Liu, S. Sun, X. Sun and Q. Kong, *Colloids Surf. A: Physicochem. Eng. Asp.*, 2023, **657**, 130549.
4. G. Wen, J. Liang, Q. Liu, T. Li, X. An, F. Zhang, A. A. Alshehri, K. A. Alzahrani, Y. Luo, Q. Kong and X. Sun, *Nano Res.*, 2021, **15**, 972–977.
5. G. Wen, J. Liang, L. Zhang, T. Li, Q. Liu, X. An, X. Shi, Y. Liu, S. Gao, A. M. Asiri, Y. Luo, Q. Kong and X. Sun, *J. Colloid Interface Sci.*, 2022, **606**, 1055–1063.
6. L. Ouyang, X. He, S. Sun, Y. Luo, D. Zheng, J. Chen, Y. Li, Y. Lin, Q. Liu, A. M. Asiri and X. Sun, *J. Mater. Chem. A*, 2022, **10**, 23494–23498.
7. H. Wang, F. Zhang, M. Jin, D. Zhao, X. Fan, Z. Li, Y. Luo, D. Zheng, T. Li, Y. Wang, B. Ying, S. Sun, Q. Liu, X. Liu and X. Sun, *Mater. Today Phys.*, 2023, **30**, 100944.
8. N. Q. Tran, L. T. Duy, D. C. Truong, B. T. Nguyen Le, B. T. Phan, Y. Cho, X. Liu and H. Lee, *Chem. Commun.*, 2022, **58**, 5257–5260.
9. H. Zhang, G. Wang, C. Wang, Y. Liu, Y. Yang, C. Wang, W. Jiang, L. Fu and J. Xu, *J. Electroanal. Chem.*, 2022, **910**, 116171.
10. Y. Li, X. He, J. Chen, X. Fan, Y. Yao, L. Ouyang, Y. Luo, Q. Liu, S. Sun, Z. Cai, S. Alfaifi, J. Du, B. Zheng and X. Sun, *Chem. Commun.*, 2023, **59**, 10805–10808.
11. Y. Zhang, Y. Wan, X. Liu, K. Chen and K. Chu, *iScience*, 2023, **26**, 107944.